Defence Technology 44 (2025) 67–82

Contents lists available at ScienceDirect

Defence Technology

journal homepage: www.keaipublishing.com/en/journals/defence-technology

Exploring the effects of angle of incidence on stabbing resistance in advanced protective textiles: Novel experimental framework and analysis

Mulat Alubel Abtew [a, *], François Boussu [b], Irina Cristian [c]

[a] University of Missouri, College of Arts and Science, Department of Textile and Apparel Management, Columbia, MO, 65211, USA
[b] Lille Université, ENSAIT, GEMTEX Lab., 2 All. Louise et Victor Champier, 59056, Roubaix, France
[c] Gheorghe Asachi Technical University of Iasi, Faculty of Industrial Design and Business Management, Str. Prof. Dr. Doc. Dimitrie Mangeron, No. 29, Iași, 700050, Romania

A R T I C L E I N F O

Article history:
Received 1 May 2024
Received in revised form
23 July 2024
Accepted 8 August 2024
Available online 14 August 2024

Keywords:
2D/3D woven fabrics
Impact protective fabric
Drop tower perforation test
Stab resistance testing protocol
Angle of incidence
Multi-layer panels
Soft body armor
Impact surface damage

A B S T R A C T

Despite numerous research investigations to understand the influences of various structural parameters, to the authors' knowledge, no research has been the effect of different angles of incidence on stab response and performance of different types of protective textiles. Three distinct structures of 3D woven textiles and 2D plain weave fabric made with similar high-performance fiber and areal density were designed and manufactured to be tested. Two samples, one composed of a single and the other of 4-panel layers, from each fabric type structure, were prepared, and tested against stabbing at [0°], [22.5°], and [45°] angle of incidence. A new stabbing experimental setup that entertained testing of the specimens at various angles of incidence was engineered and utilized. The stabbing bench is also equipped with magnetic sensors and a UK Home Office Scientific Development Branch (HOSDB)/P1/B sharpness engineered knives to measure the impact velocity and exerted impact energy respectively. A silicon compound was utilized to imprint the Back Face Signature (BFS) on the backing material after every specimen test. Each silicon print was then scanned, digitized, and precisely measured to evaluate the stab response and performance of the specimen based on different performance variables, including Depth of Trauma (DOT), Depth of Penetration (DOP), and Length of Penetration (LOP). Besides, the post-impact surface failure modes of the fabrics were also measured using Image software and analyzed at the microscale level. The results show stab angle of incidence greatly influences the stab response and performance of protective textiles. The outcome of the study could provide not only valuable insights into understanding the stab response and capabilities of protective textiles under different angle of incidence, but also provide valuable information for protective textile manufacturer, armor developer and stab testing and standardizing organizations to consider the angle of incidence while developing, testing, optimizing, and using protective textiles in various applications.

1. Introduction

Recently not only ballistic threats but also an increased number of attacks using knives, sharpened instruments, screwdrivers, and syringes has been widely reported. Among the different stab threats, cut, spike and puncture are considered the most difficult threat because it creates continuous damage by the cutting edges during the stab event. This assault becomes more serious for vulnerable personnel working in correctional institutions and first responders including enforcement officers, bus drivers, ambulance and correctional officers, bodyguards, etc. [1,2]. Even though most modern and traditional ballistic armor packages offer some degree of anti-stab protection, it is not usually claimed that ballistic armor is stab proof. Besides, stab protecting gears has been used for centuries made from different traditional stab resistant materials such as metallic chain, paper, titanium foil layers and other rigid materials such metallic sheets, ceramics, and composite plates,

* Corresponding author.
E-mail address: m.abtew@mail.missouri.edu (M.A. Abtew).
Peer review under responsibility of China Ordnance Society

https://doi.org/10.1016/j.dt.2024.08.003

polymetric structure inspire by natural structure such as scales [3]. However, developing, testing and investigating an advanced stab resistance material for protective armor has been a focus of substantial interest by various researcher for the past few decades [4–6]. The stab capabilities of those protective textiles could be influenced by various parameters. This section discussed about different research which deals with the effects of various endogenous (including material type and properties, fabric type, structure and compositions, material chemical treatment and coating) and exogenous parameters (such as testing conditions, impact velocity and energy, blade shape and types, angle of incidence and so on) on the stab response and performances of protective textiles. The effect of those different parameters on stabbing performances of the materials were conducted based on various standards, mainly National Institute of Justice (NIJ) [7] and UK standard: Home Office Scientific Development Branch (HOSBD) [8]. Angles of incidence is another exogenous parameter which could significantly impact the stabbing response and performances of protective materials by varying levels of stress and deformation on the material. Despite the above standards have recommended testing of the stab protective textile materials at [0°] and [45°] angle of incidence, to the authors' knowledge, no researcher have evaluated the effect of different angles of incidence on the stabbing response and performance of different protective textiles.

The current paper proposed a novel and unique experimental set up and methodology for testing and evaluation of several angle of incidence effects on the different 3D fabric structures and 2D plain weave high performance protective textiles. Three different structures of 3D woven fabrics were engineered and manufactured. A total of eight samples, one composed of a single and the other 4-panel layers, were prepared from each structure of 3D woven (f1, f2, and f3) and 2D plain weave (2D) high-performance fabrics were also prepared. The experimental stab testing was carried out under conventional drop tower for impact using a highly reproducibility testing apparatus. Besides, the testing bench was customized to accommodate the different stabbing angle of incidences following the HOSBD standard procedure. The apparatus uniquely applied a damped drop mass with specific and standardized blades/HOSDB/P1/B sharpness knife/dropped onto an unclamped fabric which is placed on the backing material made of standard plastiline clay 'no 1'. All the applied characteristics of the experiment including masses, velocities, and damping have been designed to mimic the biomechanics of stabbing attacks, which have been studied and proposed by different researchers [9–13] The stabbing response and performances of each fabric specimen were complemented using variables such as Depth of Trauma (DOT), Depth of Penetration (DOP), Length of Penetration (LOP) which were analyzed and discussed for the tested fabrics. The Trauma and penetration volumes were carefully printed by pouring the silicone 'RTV 181' + catalyst compounds after the test. The prints were then scanned, digitized for precise measurement of impact volume, length, width, and depth. The study also used macroscale photographs to analyze the impact surface failure modes mechanisms of the fabrics.

2. Literature review

The type and properties of the materials will be the one that significantly affects the stab response and performances of the protective gear. For instance, the effects of hybrid fibers such as aramid, basalt, and steel fibers on the stabbing performances of body protective armor has been investigated [14]. It involves various parameters including fabric density, fiber type, number of layers, fabric weight on the tested specimens and the result shows that the penetration depth decreases with the higher number of layers, the thickness, and the mass of the armor sample even though it varies according to the material type. Other research also examines the effects of fibre type (Kevlar®, Vectran®, and Spectra®), weave architecture (plain, 3/1 twill, and 2/2 twill) and stabbing direction on the quasistatic stab resistance of woven fabrics. The result reveals that Spectra® and plain weave demonstrated the highest stab resistance and further insights that fibre type, weave architecture and stabbing direction have significant roles ($p < 0.05$) in determining the stab resistance of woven fabrics [15]. Various researchers have also investigated the influences of fabric types, structure and panel arrangement on their stabbing response and performance. With this regard, apart from its good ballistic performance [16–19], mouldability and flexibility properties [20–22], 3D warp interlock structure becomes very interesting to the low-velocity stab protection [23,24]. Another research also tested and investigated the stab resistance of a warp-knitted spacer fabrics using low-twist ultra-high molecular weight polyethylene fibers and polyester monofilaments to understand the relationship between stab performance and fabric density, thickness, and the spacer structure [25]. Based on penetration force versus penetration depth result, thickness and density of warp knitted spacer fabric and the compressive property of the spacer layer structure were the main influencing factors on the stab resistance. Another study also develops double-faced knitted p-aramid fabrics with and without inlay yarns of tuck stitches of similar back and front faces and compared with jersey and plush structures having same fibers for stab performances test. The results revealed that the new structure with inlay yarns shows better cut and stab performances than other structures of similar mass per unit area and thickness values [26]. An experimental investigation on different single and multilayer triaxial weave fabrics (TWF) made of Kevlar 29, Vectran, and polyester fiber and polyester knitted, and woven fabrics were also compared to develop improved stab resistance body protective vests. Fiber index was developed to evaluate its capability to absorb the impact energy using punching resistant mechanism and low velocity punching-resistant performance testing methods. The result shows Vectran fiber with triaxial weave demonstrated higher values of energy absorption when used in multilayer fabrics along with flexibility and comfort [27]. Another study also shows an improvement in absorbed knife impact energy by reducing slippage of the yarns inside the panel layers. This was achieved by placing a layer of wool fabric on the top of the aramid panel. The standard experimental test and optical evaluation using a digital microscope showed that even though the results are also dependent on the properties and pattern of the aramid fabrics, wool can increase the stab resistance of body armor panels [28]. Another study used a multi-layer pad, highly preformed woven nets and triaxial fabrics as supporting layers to improve the puncher resistance of protective fabric. The results indicate that the specific puncture load is highest when using a silk stuffed pad supported on high tenacity polyester net. Multi-layer silk fabric over para-aramid triaxial weave fabric is superior to para-aramid plain weave fabric [29]. Other researchers also studied the effect of the aramid core-spun yarns on the stab resistance properties of the woven fabrics. Aramid core-spun yarns with core to sheath weight ratio of 1–2.5 armor specimens with different fabric densities were prepared and tested for knife impact test. The test results demonstrated that fabric density of the panel could affect the stab resistance significantly. The penetration depth of the impactor was associated with the thickness and mass of the armor sample in different ways. The stab resistance based on penetration depth of the impactor was associated with the thickness and mass of the armor sample, where there was an optimal level of the fabric density which reveals the most effective stab resistance [30]. Another study claimed that the effects of fabric elasticity and tension applied are considered as the major factors influencing the severance profile in the fabric resulting from a stab attack [31].

Chemical treatments and finishing of the protective textiles using various methods/solutions including thermoplastics [32–34], carbon nanotubes (CNT) [35], shear thickening fluid (STFs) [36–39], silica nanoparticles (SiO_2) [40], or combinations of the above [40,41] are also greatly influences the anti-stabbing properties of different protective fabric. Researchers investigated thermoplastic-Kevlar (TP-Kevlar) composites and thermoplastic (TP) impregnated woven aramid fabric against static and dynamic puncture resistant to tackle the low puncture resistance properties of Kevlar fabrics [42,43]. Both fabric solutions revealed better puncture resistance than their respective neat fabrics. Other researchers also investigated the effects of treatment and impregnations of colloidal, discontinuous STFs on different high performance fabrics in different forms with their stab response and performances [44–47]. The influences of the shear thickening fluid types on the knife stab and puncture resistance performance has been also investigated using a series of the STF enhanced fabrics [48]. The result shows that knife stab resistance performance of the STF strengthened fabric was dominated by hardness of the STF particles and the fabric strengthened by the SiO_2 based STF exhibited the highest knife stab resistance. However, fully STFs impregnated panels with larger nanoparticle size and higher weight fraction show better stab resistant performance in terms of maximum load and total energy absorption. Similarly, different study also proved that the knife stab resistance of STF threated soft ballistic body armor fabrics with different parameter exhibit significant improvements over neat fabric targets of equivalent areal density [49,50]. Another study also studied the effects of shear thickening gel (STG) parameters, including reaction time, reaction temperature, and reaction ratio, on the rheological characterization and mechanical properties of four-layer regular angle interlocking fabrics (AIF) composites. The results show that the increase in STG parameters accelerated the formation of B-O crosslink bonds within the STG and increased the energy storage modulus of STG by three orders of magnitude for a reaction temperature of 230 °C, a reaction time of 9 h, and a reaction ratio of 12.5% [51].

Some researchers have also investigated the effects of various exogenous parameters toward the stab performance and responses of different soft protective textiles. For instance, a research has studied the geometry type of the blade's stabbings influence on the effectiveness of the penetration, once the sharpness of the cutting blade and angle of the blade stabbing tip favors the impact [52]. Another research also investigated the penetrating severance damage and the stab hole size and shape during stabbing process [53]. A comprehensive analysis was conducted to evaluate the cutting performance of knife blades and the cutting depth of paper cards containing SiO_2 particles by steel blades based on a quantitative model [54]. Another study has also been carried out to determine the effect of blade handle size and shape on the forces and impact energy that could be produced during stabbing of an armored target. The result showed that the single largest variable was that of the test participants with all other variables such as handle size and shape having only slight effects on the magnitude of impact energy [9]. The effects of the impacting media, stab and puncture and the shear thickening fluid types was carried on the developed shear thickening fluid enhanced fabric [55]. The result revealed that the hardness of the particles was the dominant factor for the knife stab resistance, while the inter-yarn friction played a critical role for improving the puncture resistance. The influence of fabric structures and stab angles on single pass stab impact and the repeated and multi-angle stabbings of 3-dimensional (3D) warp interlock structural fabrics based on the high-molecular-weight polyethylene (HMWPE) yarns has also been investigated [23]. Another research also tried to investigate the effects of the number of layers, the impact energy, and the sample size on the stabbing behavior of stratified panels made of aramid fabric Twaron SRM509 Teijin Aramid BV (Arnhem, The Netherlands) [56].

3. Materials and methods

3.1. Materials

To investigate and understand the effect of the angle of incidence during stabbing of soft textile materials, three different architectures of 3D woven fabrics, named as f1, f2, and f3 onwards were designed and manufactured. While manufacturing, all the 3D warp interlock fabrics (3D WIFs) were engineered with same architecture (O-L-Orthogonal Layer-to-Layer), number of weft layer (five weft layers), yarn types (high performance p-aramid with 930 dtex and 25 twists/m yarn with Z direction twist) but different warp yarn binding structures. The average thickness of the five-layer 3D WIFs recorded in a range of 1.42–1.62 ± 0.35 mm for the different architecture with same mass per unit area of 970 ± 5 g/m^2. Besides, the commercially available Twaron CT-709 2D woven fabric by Teijin Aramid, named as 2D onwards, made of similar yarn type, and composition with the manufactured 3D WIFs were also used in the study for comparison. A one ply of 2D woven fabric measures 0.3 ± 0.35 mm thickness (5 ply of 2D will have 1.5 ± 0.35 mm thickness) and its areal density was also of 970 g/m^2 for five ply fabrics. The general definitions of the different proposed 3D WIF structures are described below.

- 3D WIF - Orthogonal layer-to-layer (O-L) 5 1–2 4 Binding {Plain weave} - 0 - Stuffer (f1 fabric)
- 3D WIF - Orthogonal layer-to-layer (O-L) 5 1–2 4 Binding {Plain weave} - 4 - Stuffer (f2 fabric)
- 3D WIF - Orthogonal layer-to-layer (O-L) 5 1–4 4 Binding {Plain weave} - 4 - Stuffer (f3 fabric)
- 5 layers of 2D-woven fabric, plain weave (2D fabric)

The intended 3D warp interlock fabric structures were produced with controlled conditions using a semi-automatic and customised ARM dobby weaving machine. To produce a lower degraded 3D fabric, the machine was set-up with the twenty-four shafts where each Heald shaft were engaged and corresponds with one warp beams. The weaving systems were also equipped with a horizontal bar with guiding hole to accommodate and passing each warp yarn to the weaving zone to avoid overlapping and friction among one to other. The average thickness of the preforms were precisely measured using SODEMAT textile micrometre with electromagnetic sensor to determine the distance between the two plane surfaces under the action of an adequate mass with the good precision (approximately 3%) according to ASTM D 1777–96 (2007) [57]. The geometrical structure of the proposed architectures is shown in Fig. 1.

3.2. Sample preparation, stab testing principles and stab impact measurement

3.2.1. Sample preparation

A total of eight variants of test specimens, which comprises two distinct categories based on their number of layer composition were prepared. For example, the first four samples comprising a total of 5 weft yarn systems and the other four samples made from a total of 10 weft yarn systems from each fabric types (f1, f2, f3, and 2D). The first four samples made from a single panel (5 weft yearn systems) of each 3D woven fabrics (f1, f2, and f3) and the 5 layers of 2D woven fabric are designated as [f1]1, [f2]1, [f3]1, and [2D]1

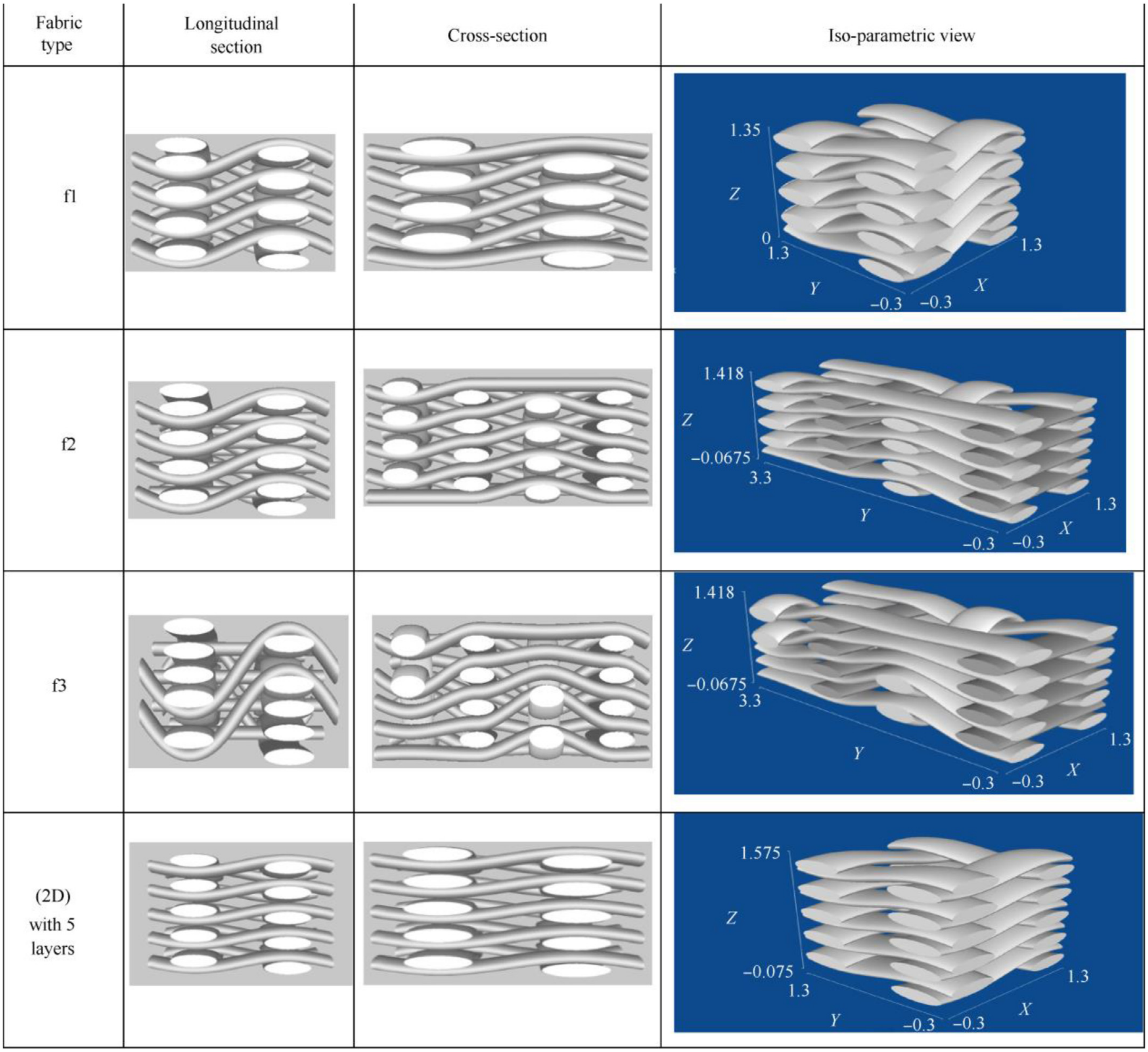

Fig. 1. The geometrical structures of the different 3D WIFs {f1, f2 and f3} and 2D plain weave fabric {2D} architecture.

respectively. The other four sample which are made from four layers of each 3D woven fabrics (f1, f2 and f3) and twenty layers of 2D woven fabrics are designated as [f1]4, [f2]4, [f3]4, and [2D]20 respectively. Each sample in their respective categories have an equivalent areal density. For example, samples {[f1]1, [f2]1, [f3]1, [2D]1} and {[f1]4, [f2]4, [f3]4, and [2D]20} have an areal density of approximately 970 and 1940 g/m^2 respectively. All the samples were precisely cut using an electric cutter dedicated for high performance fabrics and prepared with squared 100 mm × 100 mm operating areal dimensions for stab resistance test as shown in Fig. 2(a). The stab test was repeated five times for each of the eight types of protective fabrics. Since the results of stabbing behaviours of textile materials can be greatly affected by the amount of moisture present in the materials, the sample specimens were kept under standard conditions of relative humidity (65 ± 4.0%) and temperature (20 ± 2.0 °C) as recommended by ISO 139–2005, prior and during the test. This is due to the change of environment humidity could strongly influence the stabbing behavior of the tested fabric because of the modification of the friction behavior between the stabbing tool and the textile materials. Unlike a single panel sample, the four panels' samples of each fabric type were aligned together and finished using scotch tape only at the edge with same yarn direction (0°) before testing as shown in Fig. 2(a).

3.2.2. Drop tower stab testing equipment and testing procedures

The drop tower impact test system was used to test the stabbing performances of the specimen as shown in Fig. 3(a). The test was carried out according to the UK Standards: Home Office Scientific Development Branch (HOSBD) which is the standard stab test for protective armor. The test was carried out under the principle of falling of blade knife in specified height with its own weight influence (gravity) to generate energy for impact. The stab testing

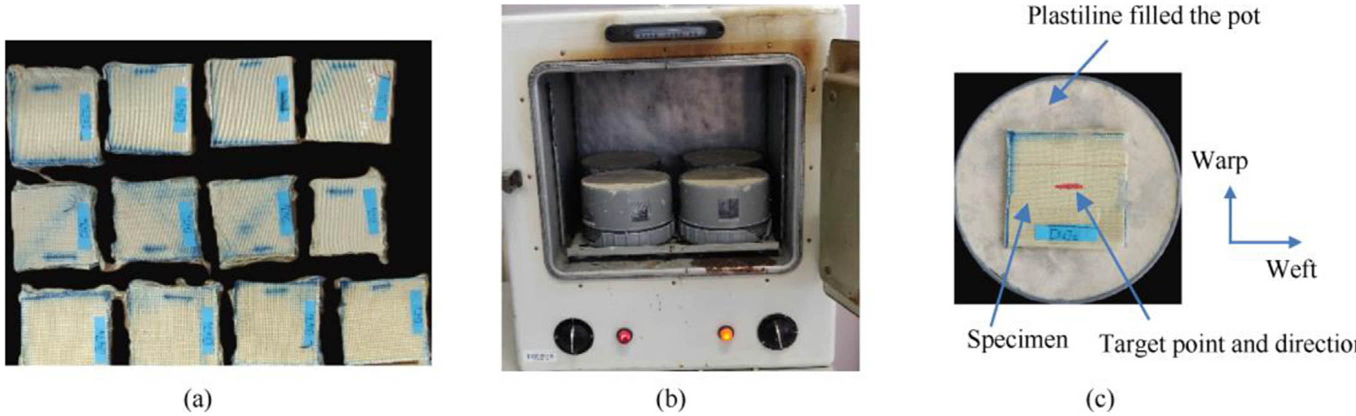

Fig. 2. (a) Some of the prepared specimens from different fabric types; (b) Electric oven for temperature regulations of the backing material; (c) Specimen set on the top of backing materials/plastiline holder pot ready for the stab test.

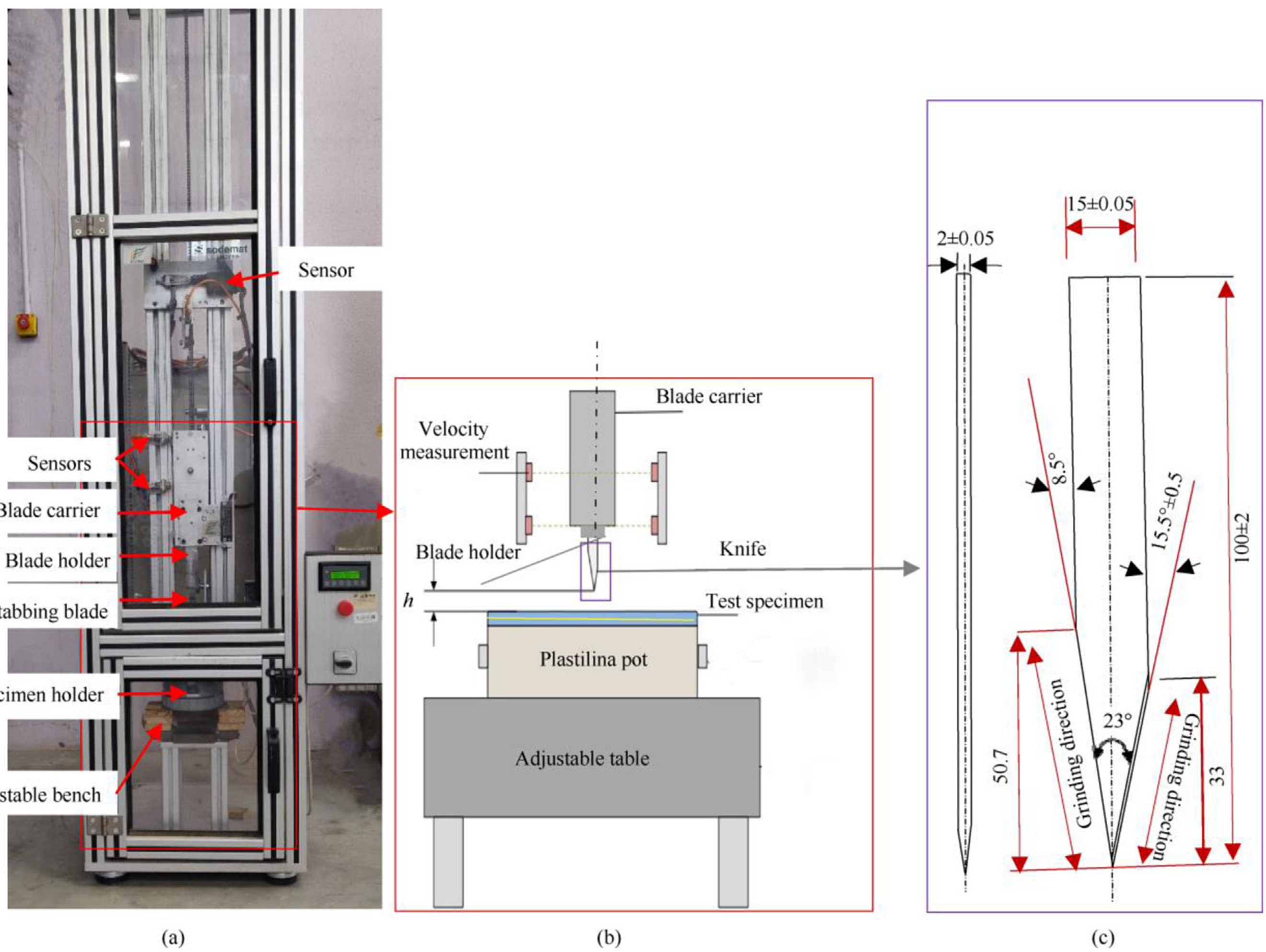

Fig. 3. Stabbing tests experimental system: (a) Photograph; (b) Its schematic view of the stabbing test bench; (c) Detailed elements of the schematic diagram of the HOSDB P1B knife blade for stabbing test (dimension in mm).

machine mainly consists of three main parts namely the galvanized aluminum frame, the carriage, and the sample support. The frames are responsible for holding two vertical rails to guide the carriage, sample support and all the accessories used for automation. The carriage is also used to support and fix the different blade types in its lower part. Even though the mass of the carriage unit is fixed for different blade types, its mass can also be increased by adding some weights on the support to adjust the required energy for impact. The blade is fixed to a carriage that carries tools which can slide along two vertical rails by means of a connection slide with negligible friction. The height of release as well as the mass of the carriage can be adjusted to test several energies of impact and impact speeds. The speed is being measured by a magnetic sensor on the lower part of the perforation bench. To achieve such potential energy for the impact process, the different parameters including the falling height and mass of the impactor should be known. Then, it is determined with the assumption that the blade knife falls without creating friction forces at the rails using Eq. (1).

$$W_{\text{pot}} = m*g*h \tag{1}$$

where, W_{pot} is the potential energy, m is the mass of the blade plus the holder, kg, g is the acceleration due to gravity, m/s^2 and h is the falling height, m.

At the beginning, different impact energy 2.07, 4.76, 7.24, 12, 24 J were selected to test the specimens as preliminary test. This helps to understand the resistance capacity of the prepared specimens for better analysis. Those different potential energy were achieved by dropping a 2.11 kg base mass of the blade knife plus holder at the different falling height. The different fall height was calculated using Eq. (2) as follows:

$$h = \frac{W_{\text{pot}}}{m*g} \tag{2}$$

The different height set to generate the above impact energies, 2.07, 4.76, 7.24, 12, and 24 J, are found to be 116, 230, 350, 580, and 1160 mm, respectively. After testing, some of the larger impact energies were found to be too high for the specimen to resist, while others were too small to yield visible differences among the specimens after testing. Thanks to this preliminary result, a constant impact energy of 7.24 J, where a 2.11 kg blade knife plus holder falls from a height of 350 mm, was found appropriate for assessing each specimen to identify differences between the various fabric specimens and understand the effect of angle of incident on their stabbing performance. An HOSDB/P1/B sharpness knife blades which have a total length of 100 mm, the edge of cutting length of 33 mm, and the blade thickness of 2 mm were used. Its detailed descriptions and dimensions are illustrated in Fig. 3(c) [16]. Even though the study follows the UK standard: HOSDB Body Armor Standard testing procedures, the applied energy was much lower than the one considered in the standards of personal protection analysis for real armor vest due to the lesser plies of textile fabric used during the stabbing test to understand the angle of incidence effects. The backing material which consists of a particular modelling clay designed to resemble the body texture called 'Roma Plastiline® No.1' was used to support the specimen as shown in Fig. 2(c). The backing materials will receive the stab impactor during the test which aides to further analyze the stabbing performances of the materials including trauma and severity of the penetration. The backing materials were filled into a 135 mm diameter, 2 mm thickness, and 95 mm height supporting circular pot. Each supporting pot filled with the Roma Plastiline® No 1 shall be conditioned in a heated enclosure for at least 3 h at a temperature above 30 °C as shown in Fig. 1(b).

The actual conditioning temperature and recovery time between each strike has been determined through calibration based on the HOSBD standards. The width and thickness of the stabbing blade were positioned along the warp and weft yarn directions respectively as shown in Fig. 4(a). Each test specimen was kept freely on the top of backing materials, and the strike was performed at center with similar positions as shown in Fig. 4(b). Besides, the specimens were tilted along the warp direction to achieve the different angle of incidence during testing as shown in Fig. 4(c). This procedure was suggested to imitate the real scenario of stab attack on the protective vest. Apart from impact energy exerted and type of the blade used, stabbing angle of incidence could bring an effect on the final blunt trauma and penetration depth. To understand such effect, a new plastiline holder bench was designed to accommodate different angle of incidence [0°], [22.5°], and [45°] while stab testing. Angle of incidence is the angle formed between the line of flight of the drop mass and the perpendicular line to the plane tangent to the point of impact. For example, for a perpendicular stab impact, the impact angle will be 90° to surface and its corresponding angle of incidence will be [0°]. This indicated that the striking line of the blade is aligned perpendicularly to the top impact surface of the test specimen as shown in Fig. 4(b) (top picture). Other angles of incidence have been obtained by changing the positions of plastiline holder bench by changing the angle of plastiline holder bench without changing the striking positions of the blade (which is always vertical). For instance, [22.5°] and [45°] angle of incidence was achieved by tilting the customized plastiline holder with respective degree at the bottom as shown in Fig. 4(b) (middle [22.5°] and bottom [45°]). However, if the test specimen is kept at the center of the pot for different angles of incidence, the total mass dropping height could be varied. For example, the total mass dropping height for [22.5°] angle of incidence will slightly lower than that of [45°] due to a little down shift of the strike point. Such increments of the drop height could slightly increase the impact energy and might affect the comparison result. To avoid this, the position of the specimen on the backing material has been adjusted for both [22.5°] and [45°] angle of incidence to achieve same total drop height as [0°] angle of incidence. By this way it is possible to have the same impact energy applied for all specimen at different angles of incidence. Moreover, similar principles were considered while testing specimens having different thickness for better comparison. Fig. 4(c) shows the schematic diagram of the line of the knife blade impact of the test specimen at different angles of incidence.

3.2.3. Stab resistance measurement systems

During stabbing of soft textile materials, the knife first damages the material and then creates either a trauma, perforation or/and penetration at the back. Such phenomenon could be affected by different parameters including type and parameters of materials, type of the knife, the striking energy, impacting angle etc. In this study, the influences of different angles of incidence on the performances of materials based on deformation created at the back and fabric damage are investigated. During perpendicular [0°] impact of the materials, two possible behaviors at the backing material could occur according to the reaction of the protective textile. Such stabbing depth can be divided into two parts, depth of penetration (DOP) and depth of trauma (DOT) as shown in Fig. 5(c). The two values could be directly measured from the backing materials. The DOT measures between the top surface of the fabric till the beginning of the penetration surface. On the contrary the depth of trauma (DOP) is the distance between the start of the penetration point to the bottom tip of the blade. On the other hand, the stabbing depth will be different when the specimen stroked with an angle, for instance [22.5°] and [45°]. Unlike the perpendicular impact [0°] angle of incidence, the angled strike (θ) will possess two different kinds of trauma depth in either side of impact, namely the shorter depth, DOTs, and the longer depth DOT_l as shown in Fig. 5(d). The longer trauma depth (DOT_l) will be created on the side where more blade surface is in contact with the specimen and backing material. Besides, there are two measurements for penetration of the blade knife. The first is the perpendicular distance measured from the top surface of the fabric, where penetration started to the tip of knife blade. The other, length of penetration (LOP), is the total slant length of penetration along the edge line of the blade knife. Penetration width (PW) is the widest width created by the knife during penetration. Such width of penetration occurs

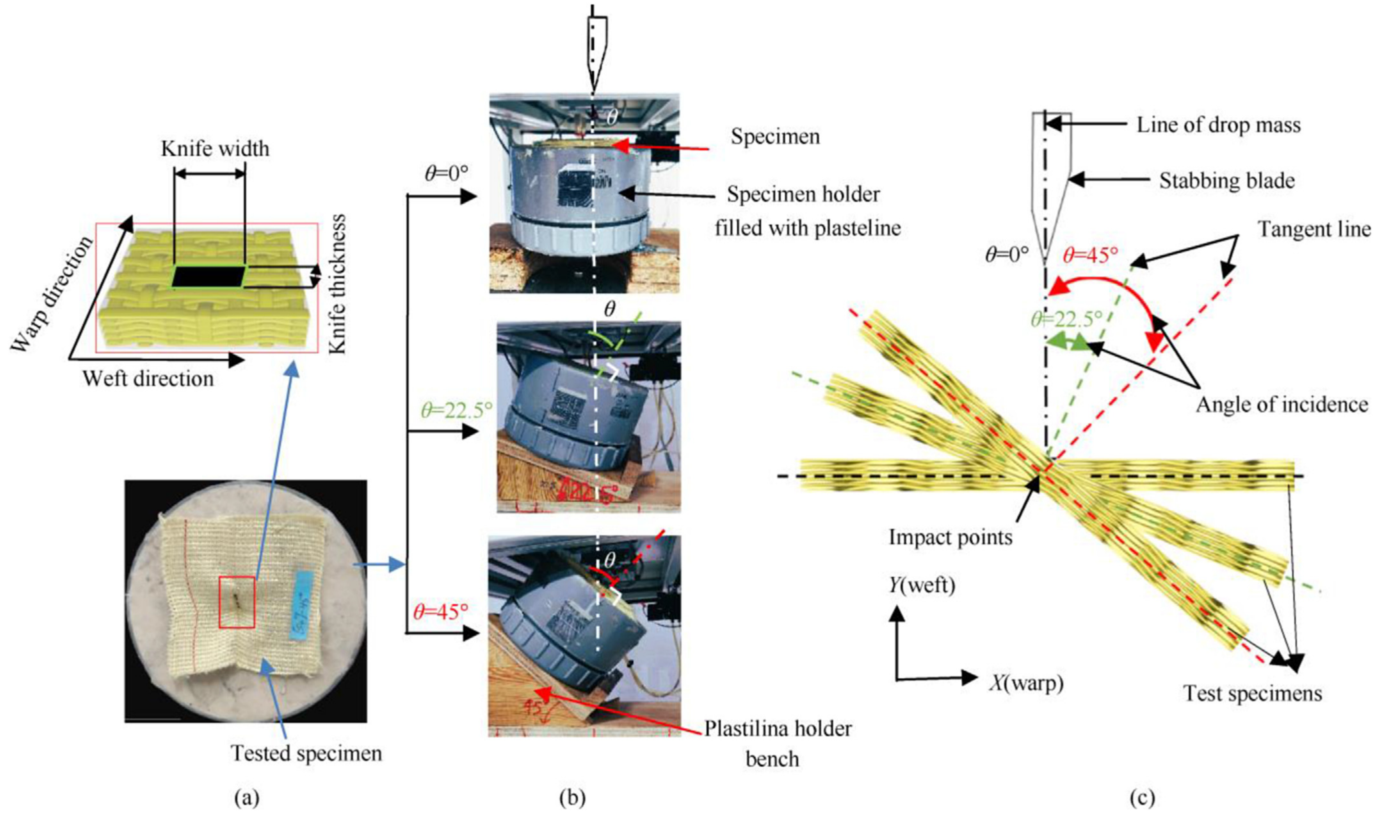

Fig. 4. Stab testing procedure: (a) Tested specimen and the direction of stabbing knife with respect to the yarn direction; (b) Positioning of the specimen holder; (c)Its schematic view of stabbing and impact position of the test specimen at different angle of incident ([0°], [22.5°], [45°]).

mostly at the beginning of the penetration. Following each stab test, the specimen holder pot filled with Roma Plastiline® No.1 will be taken out from the stabbing bench and placed on a horizontal plain surface. Subsequently, the tested specimen will be carefully removed from the backing material to prevent damage to both the deformed backing material and the specimen. This procedure ensures accurate stabbing deformation measurements and maintains the integrity of the specimens for further analysis. After removing the tested specimen, the backing material with stab deformation is kept at room temperature. Fig. 5(a) depicts the top surface and its Back-Face Signature (BFS) state of the Plastiline® after stabbing impact. Different high division scales like Vernier caliper or digital microscope methods could be also employed to measure stabbing deformation such as DOP, DOT, trauma diameter after stabbing. Besides, due to its convenience and better accuracy, other researchers have also used silicon to capture the final shape of the blade and fabric deformation into the plastiline for measuring the various trauma variables directly on it [23].

Subsequently, the mixed silicon compound was carefully poured dropwise with the spatula into each deformed plastiline as shown in far-right picture in Fig. 5(b) to obtain the required prints of the trauma (Fig. 6). During pouring, it is also very crucial to ensure that the silicon compound completely flows into the deformed hole and fills the trauma completely and accurately up to the top surface edges of stab deformation. Besides, like plastiline preparation, it is also very important to avoid air bubbles emerging while pouring the silicon compound to the deformed plastiline during the test. After pouring into the trauma, the silicon compound should stay in the backing plastiline hole for approximately 30 min for curing before further measurement and analysis. Once the silicon print was obtained, it was possible to scan it in 3D, transfer to the 3D Design concept software and precisely measure the different trauma variables less than 0.01 mm error as shown in Fig. 6.

For example, in the case of perpendicular impact (0° angle of incidence), the Depth of Penetration (DOT) can be easily measured by determining the distance between the top surface of the silicon print and the beginning of the penetrated material (Fig. 6(a)). Additionally, the maximum surface deformation or damage diameters of the BFS can also be measured both in the knife width (X_{max}) and thickness (Y_{max}) direction by assessing the top surface of the silicon print as shown in Fig. 6(a). While the material's stab resistance is primarily determined by the Depth of Penetration (DOP), where a higher penetration depth indicates lower stab resistance [16], this relationship may not hold true in cases involving angled impacts. This discrepancy arises because, unlike perpendicular impacts, the Length of Penetration (LOP) does not necessarily match the Depth of Penetration (DOP), as illustrated in Fig. 6(c).

4. Results and discussion

While the perforation of the textile fabric by the blade, there will be two possibilities, the first is when the anti-perforation protection is rigid (there is no displacement of the modelling clay) and the second one is if the anti-perforation protection is flexible, where there is displacement of the modelling clay. In this study, the sample material is flexible and follows the perforation of a flexible structure as shown in Fig. 5.

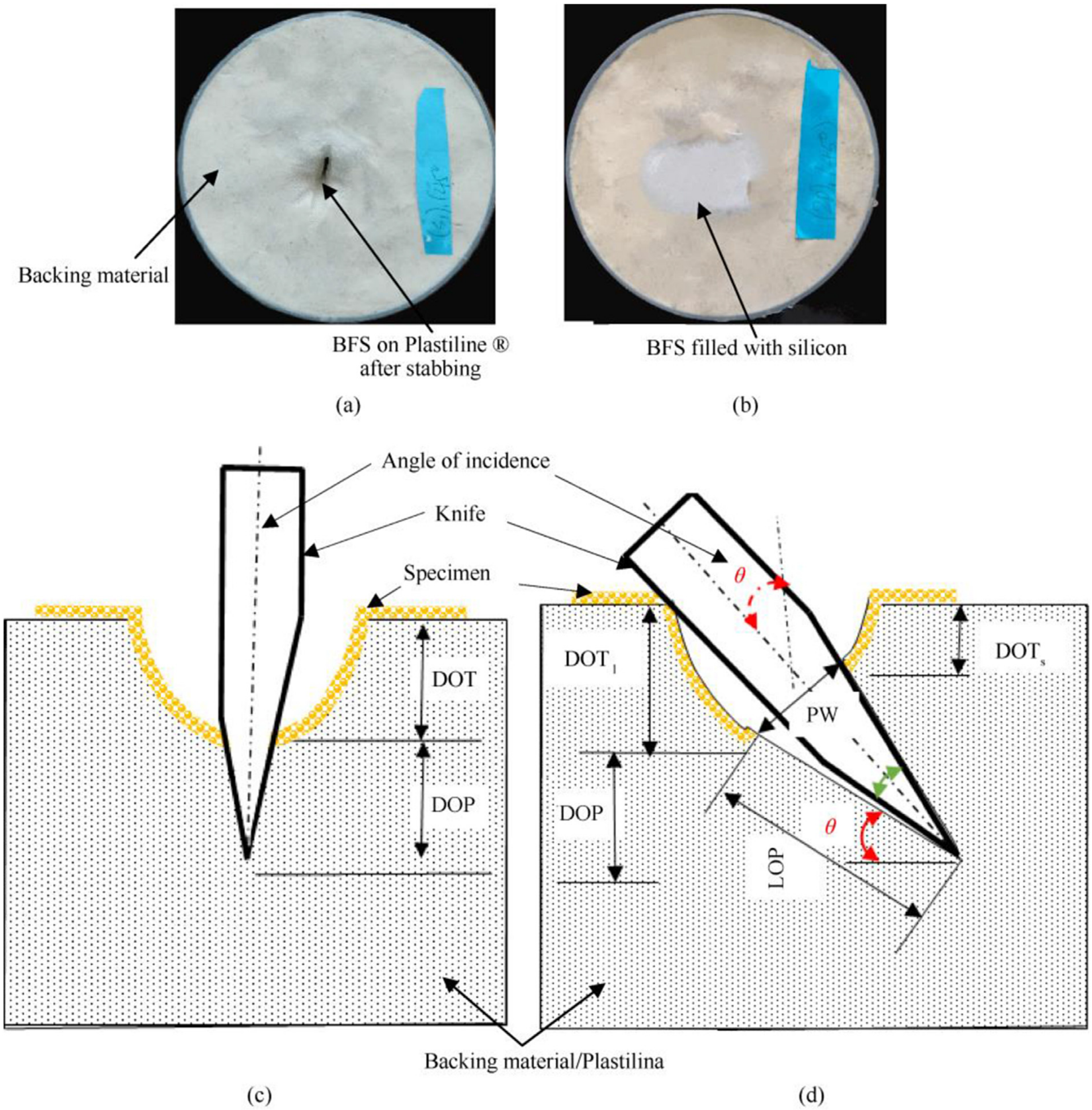

Fig. 5. The Back-face signature (BFS) deformational principle during stabbing test: (a) The back-face signature (BFS) or deformations of backing materials after stabbing; (b) Filling of the backing material deformation with Silicon to print the BFS; (c) Schematic diagrams during stabbing to show the deformation of trauma (DOT) and penetration (DOP) at perpendicular stabbing (0°) and (d) at angled (22.5° or 45°) stabbing.

4.1. The effect of angle of incidence and fabric structure on stabbing performances

In general, three different stages might occur while the knife attacks the protective materials. First it creates indentation on the back of the surface, second it will perforate the materials surface, then lastly will create penetration. However, the number of different stages created will depend on the amount of energy exerted by the knife and/or the performance of the protective materials. Therefore, in some cases, there is only either one stage, indentation, or two steps, indentation, and perforation, might occur during stabbing-resistant materials that they do not been penetrated by the knife during the stabbing impact.

To test the effects of angle of incidence and the fabric type on stabbing performance, a Two-Way ANOVA was employed. The results, presented in Table 1, indicate the statistical significance of angle of incidence and fabric types on the depth of trauma (DOT) and depth of penetration (DOP) during stabbing resistance tests. Based on the result, a p-value less than 0.05 leads to the rejection of the null hypothesis, thereby confirming the significant effect of the variables or their interaction at a 95% confidence level.

Our investigation shows that the effects of both angle of incidence and fabric type are significant, as the *P*-values for both variables are less than 0.05. For the angle of incidence, the *F*-value (1659.33) greatly surpasses the *F* critical value (3.124), with a *P*-value much smaller than 0.05, confirming its significant effect on DOT and DOP. Similarly, for fabric type, the *F*-value (583.54) far exceeds the *F* critical value (1.92), with a *P*-value much smaller than 0.05, indicating a significant impact on DOT and DOP. Additionally, the interaction between fabric type and angle of incidence is

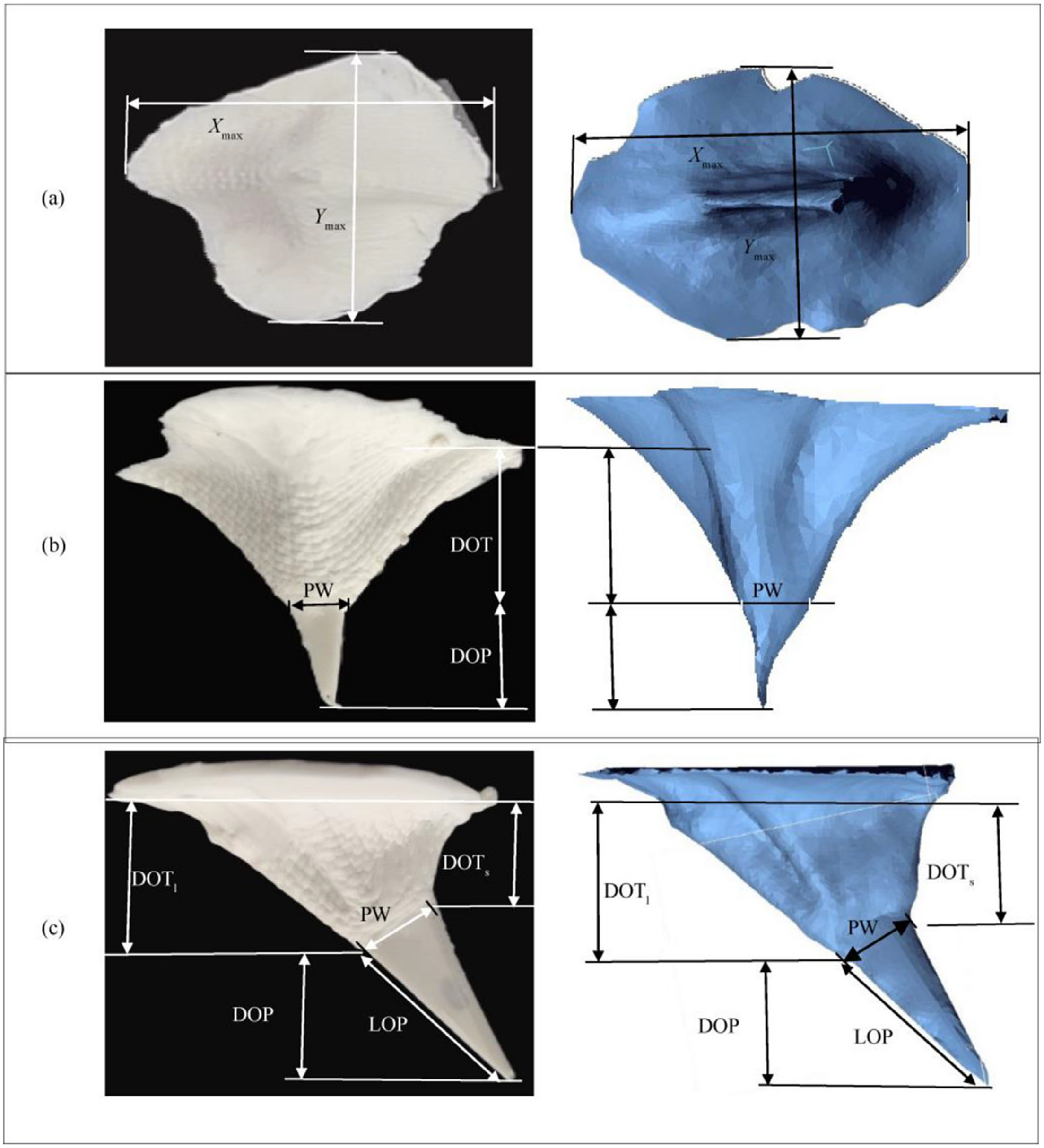

Fig. 6. (a) Top view of the maximum surface damage diameters of the BFS; (b) Side views of the perpendicular impact (0°angle of incidence); (c) Angled impact (45° angle of incidence) of stabbing deformation printed with Silicon and its corresponding 3D scanning.

Table 1
ANOVA analysis table.

Source of Variation	Sum of Squares	Degree of freedom	Mean Square	*F*-value	*P*-value	*F* crit
Fabric type	4175.42	11	379.58	583.54	1.06425×10^{-65}	1.92
Angle of incidence	2158.74	2	1079.37	1659.33	5.93947×10^{-61}	3.12
Interaction	11046.78	22	502.13	771.92	1.28915×10^{-76}	1.69
Within	46.84	72	0.65			
Total	17427.78	107				

significant, as evidenced by an *F*-value (771.93) much larger than the *F* critical value (1.69) and a *P*-value much smaller than 0.05. This interaction signifies that the effect of fabric type on DOT and DOP is dependent on the angle of incidence. In general, there is a statistically significant effect of fabric type, angle of incidence, and their interaction on the two stabbing performance metrics, DOP and DOT.

Given the significant interaction effect, further analyze was performed to understand how each fabric type behaves at different angles of incidence in respective of DOP and DOT. Fig. 7 illustrated a compelling interaction analysis on the effect of angle of incidence on stab performances measured by both the DOT and DOP for a 2D fabric (2D) and three distinct types of 3D fabrics (f1, f2, and f3). It offers crucial insights on how varying angles of attack influence the

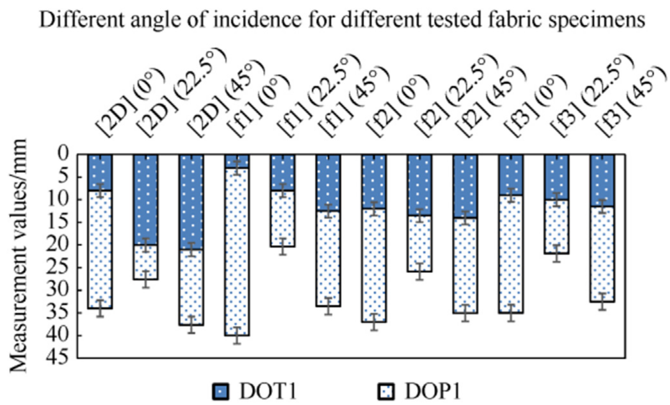

Fig. 7. The maximum Depth of Trauma (DOP1) and Depth of Penetration (DOP1) of the tested specimens made of 5- weft systems of different fabric structure with specific angle of incidences ([0°], [22.5°] and [45°]).

protective fabric's ability to withstand and mitigate stabbing forces. Firstly, the data reveals a clear trend regarding the DOT across different angles of incidence. As the angle increases from [0°] to [45°], there is a noticeable escalation in the depth of trauma inflicted on the fabrics. This observation suggests that higher angles of incidence result in greater trauma to the material, indicating a reduced ability to absorb and distribute the impact energy efficiently. The escalating DOT values underscore the fabric's increased susceptibility to damage as the angle of attack becomes more acute, highlighting a crucial aspect of material behavior under stabbing forces. On the contrary, the analysis of the depth of penetration unveils an intriguing pattern. At [0°] angle of incidence, the depth of penetration is notably high, indicating that fabrics face a significant risk of puncture and shear force when subjected to a perpendicular angle of attack. This finding aligns with the intuitive understanding that forces directly opposing the fabric's surface are more likely to penetrate deeply. Surprisingly, the data reveals that at [45°] angle of incidence, the depth of penetration is also relatively high, suggesting that acute angles of incidence can still lead to substantial penetration despite the reduced trauma depth. This phenomenon may be attributed to the nature of the force distribution and the fabric's response to oblique impacts. Remarkably, Fig. 7 also shows that at [22.5°] angle of incidence, the depth of penetration is consistently lower for all fabric types compared to both [0°] and [45°] angle of incidence. Furthermore, different stabbing impact behaviors were observed among various types of protective fabrics. For instance, at a [0°] angle of incidence, both f2 (composed of 50% binding and 50% stuffer yarn in the warp yarn system) and f3 (comprising 33.5% binding and 66.5% stuffer yarn in the warp yarn system) demonstrate better stab performance in terms of DOP, measuring 25 mm and 26 mm, respectively, compared to f1 (comprising 100% binding yarn in the warp yarn system) with a DOP of 37 mm. However, all three 3D fabrics (f1, f2, and f3) exhibit equivalent stabbing performance capabilities when tested at both [22.5°] and [45°] angles of incidence. This indicated that the involvement of stuffer yarn in the warp yarn system could enhance the shear resistances of the fabrics, which is crucial for the stab performance. This observation implies that intermediate angles of incidence offer a degree of protection against penetration, presenting an interesting finding for fabric designers and engineers. While the exact mechanisms behind this phenomenon warrant further investigation, suggesting that certain angles may optimize the fabric's ability to resist knife stabbing without compromising the overall stab performance. Based on the above result, the angle incidence on stab performances provides valuable insights into the complex interplay between fabric structure, force application, and material response. It underscores the importance of considering angle effects in designing protective textiles and highlights potential strategies for enhancing stab resistance across different angles of attack.

Fig. 8 provides a comprehensive analysis of the impact of angle incidence on stab performances, specifically measured through the length of penetration (LOP) for both 2D and three distinct types of 3D fabrics. LOP, defined as the length of penetration of the blade along its edge, serves as a crucial metric for evaluating the fabrics' resistance to stabbing forces under different angles of attack. The findings elucidate intriguing variations in LOP values across varying angles of incidence and fabric types, offering valuable insights into material behavior and performance optimization.

For the 2D fabric specimen, the analysis reveals distinct trends in LOP values at different angles of incidence. At [22.5°] angle of incidence, representing a slight acute angle of attack, the LOP values are notably higher compared to other angles. This observation suggests that the 2D fabric is more susceptible to deep penetration when subjected to direct perpendicular forces. Surprisingly, the LOP values at [45°] angle of incidence are also relatively high, indicating that a very high acute angles of incidence can still lead to significant blade penetration. However, the most intriguing finding emerges at [0°] angle of incidence, where the LOP values are found to be minimum. This suggests that intermediate angles of incidence offer a degree of protection against deep penetration, highlighting a potential optimization strategy for enhancing stab resistance in 2D fabrics. In contrast, the analysis of LOP for the 3D warp interlock fabric specimens presents a different picture. Even though the trend is similar, the LOP values of all three fabric types (f1, f2, and f3) show higher values compared to their counterpart 2D sample in their respective angle of incidences. However, the values at [22.5°], followed by [45°] angle of incidence were higher than at [45°] angle of incidence. This indicates that these fabric structures exhibit greater vulnerability to blade penetration at these acute angles of attack.

Interestingly, the LOP values are found to be lower for the perpendicular angle of [0°] angle of incidence, suggesting that three different 3D fabrics (f1, f2, and f3) offer relatively better resistance to stabbing forces when subjected to direct perpendicular impacts. Overall, the analysis of LOP values underscores the complex interplay between fabric structure, angle of attack, and stab performance. While 2D fabrics (2D) demonstrate varying susceptibility to blade penetration across different angles of incidence, the different 3D fabrics exhibit distinct patterns influenced by their specific structural characteristics. The detailed analysis of Fig. 9 provides

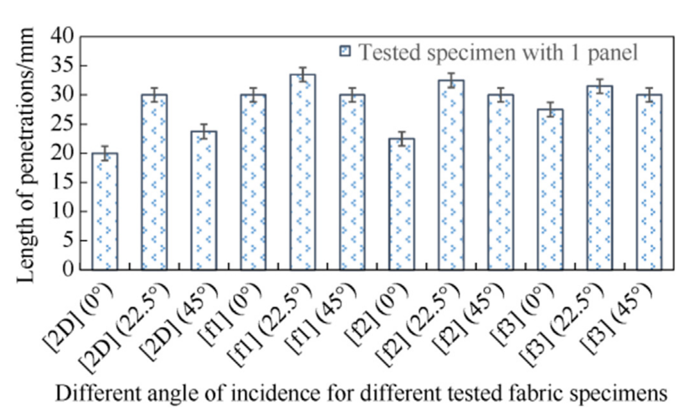

Fig. 8. The maximum Length of Penetration (LOP) along the blade edge of the tested specimens made of 5- weft systems different fabric structure with specific angle of incidences ([0°], [22.5°] and [45°]).

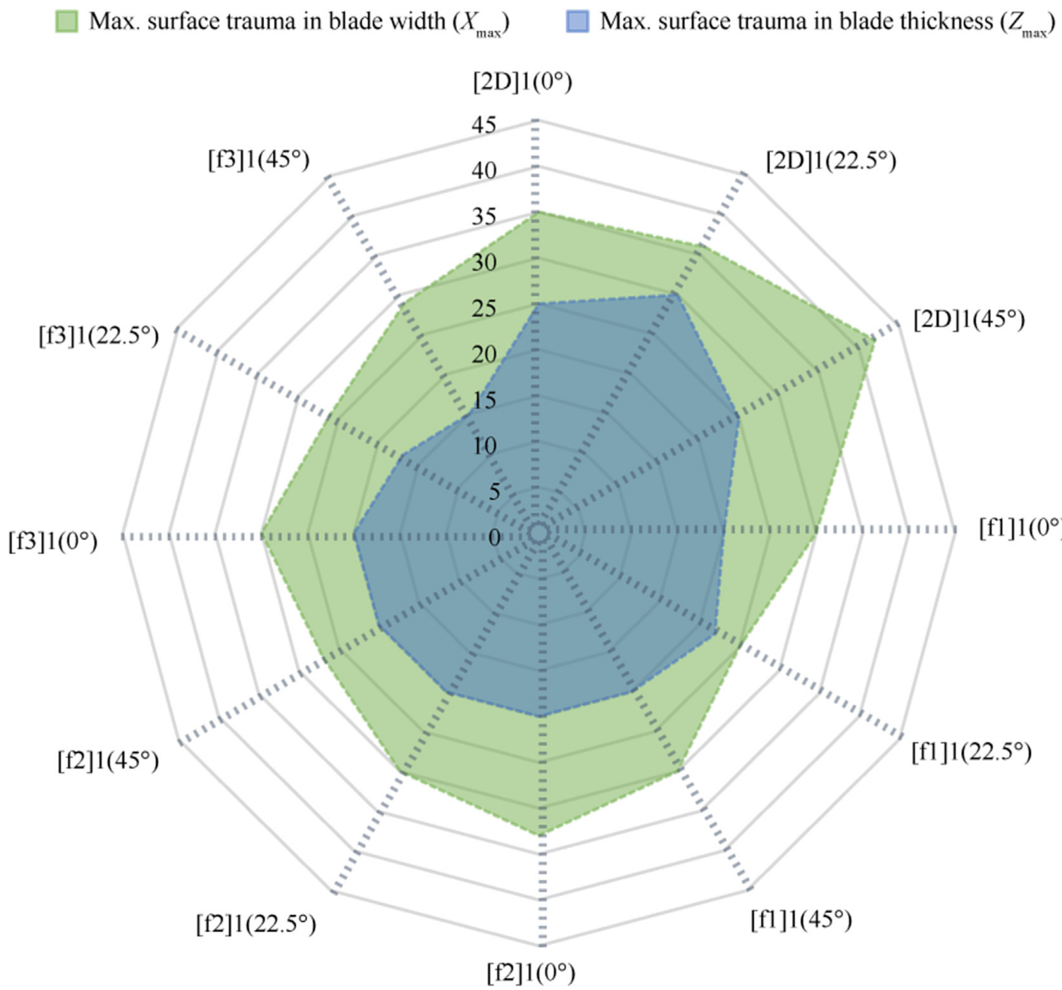

Fig. 9. The maximum trauma deformation measurement on the top surface of the backing material along the blade thickness (*Z*) and blade width (*X*) direction while testing the one panel of different fabric specimen with specific angle of incidences ([22.5°], [22.5°] and [45°]).

valuable insights into the comparisons of maximum trauma measurements on the surface of backing materials during stabbing, considering both the maximum knife width and thickness directions. By examining the effects of different angles of incidences [0°, 23°, and 45°] on various fabric specimens, including 2D and f1, f2, and f3, the analysis shows interesting patterns in trauma values and their directional preferences. One prominent observation highlighted in the analysis is the consistent trend across all specimens, where the maximum trauma surface values are consistently higher in the knife width direction compared to the thickness direction. This trend underscores the importance of fabric structure and orientation in determining vulnerability to stabbing forces, with fabrics exhibiting greater resistance along the thickness dimension. Examining individual specimen responses to different angles of incidence reveals nuanced variations in trauma surface values.

For instance, specimen 2D at [45°] exhibits a maximum trauma surface value of 42 mm in the knife width direction and 25 mm in the thickness direction. In contrast, specimen f1 at [22.5°] angle of incidence shows a maximum trauma surface value of 25 mm in the knife width direction and 22 mm in the thickness direction. This demonstrates how the angle of incidence influences trauma distribution on fabric surfaces, with varying degrees of impact intensity. Further analysis reveals a notable effect of angle of incidence on maximum trauma surface values, particularly in the knife width direction. For specimens 2D, f1, and f2, similar trends are observed, with maximum trauma surface values peaking at [45°], followed by [22.5°] angle of incidence. Conversely, the [0°] angle of incidence consistently yields minimum values for these specimens. For instance, in the knife width direction, specimen 2D exhibits maximum trauma surface values of 35 mm, 36 mm, and 42 mm at [0°], [22.5°], and [45°] angle of incidence, respectively, illustrating the impact of angle on trauma distribution. Interestingly, specimen f3 deviates from this trend, displaying similar maximum trauma surface values in the knife thickness direction across all angles of incidence. This suggests that the structural characteristics of f3 may render it less sensitive to variations in angle compared to other specimens.

Other ways of examining the effect of angle of incidence on the materials stab performance is by analyzing the post impact fabric failure mode. Fig. 10 illustrates both the side view and the specific perforated area from the bottom of the specimens. In general, when stabbing occurs, the fabric damage being caused as the blade runs along the specimen. During the impact process, part of the strike energies is absorbed by the specimen while the rest is transmitted beyond to the backing material (plastiline). Since the current study considers a single-stab test, a slash cut would not be expected to be generated by the swinging motion of the blade. As shown in Fig. 9, all the test specimens made with a single panel fabric were totally penetrated regardless of the type of fabric tested. However, the

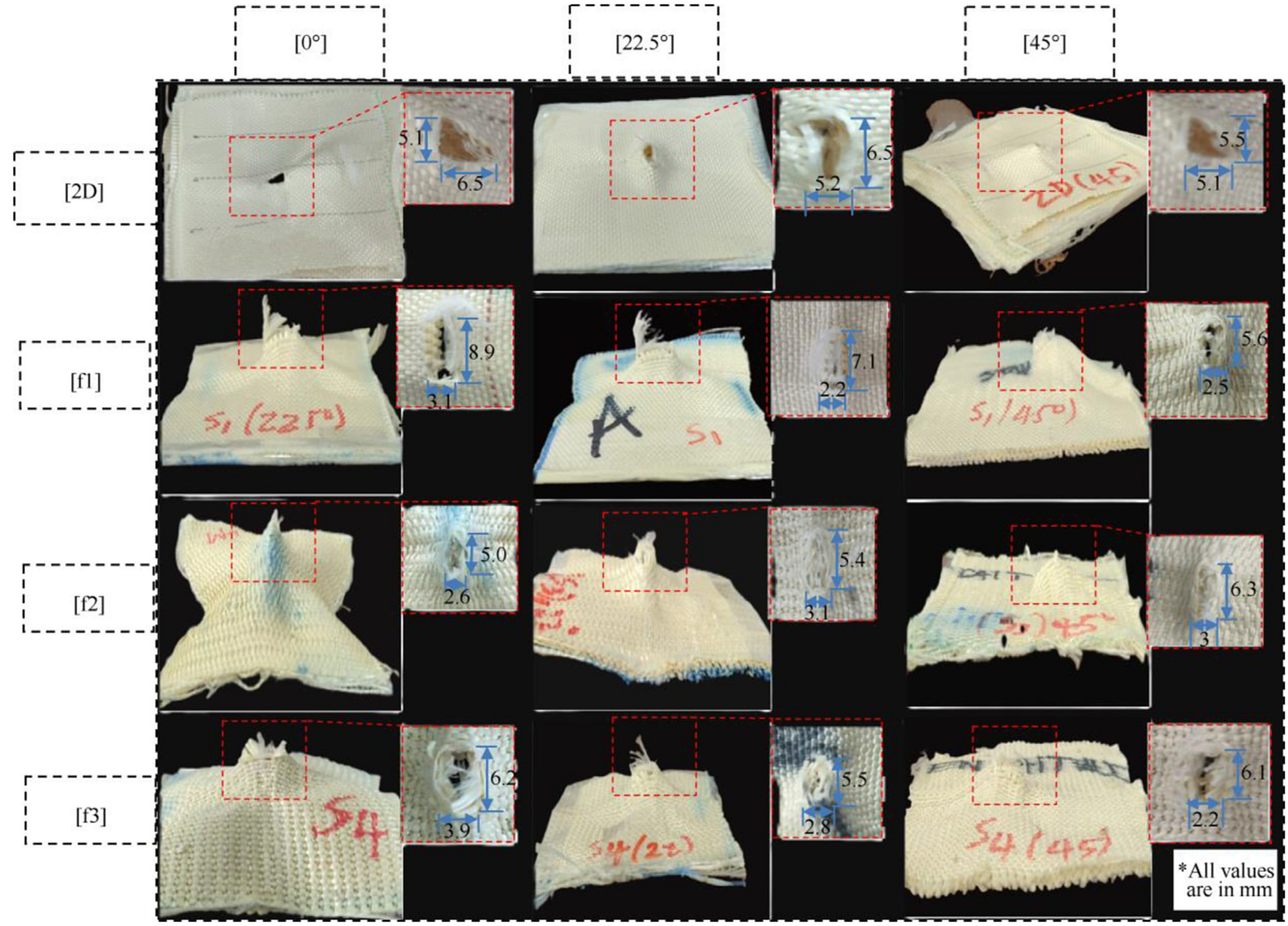

Fig. 10. The side views of tested fabric, the zoomed area at the failure area of post impact, and its measured values (in mm with ±0.05 mm error) at the knife width (vertical) and thickness (horizontal) direction of different fabric types ([2D], [f1], [f2] and [f3]) (a scale of 10 mm) made of one panel at different angles of incidence ([0°], [22.5°] and [45°]).

perforated hole on the fabric along the blade thickness was found higher at the 2D fabrics compared to all other 3D WIFs. Comparing the 3D WIFs structure, f1 specimen shows higher perforation width, 8.9 mm, and 7.1 mm both at [0°] and [22.5°] angle of incidence respectively as compared to all other fabric specimen types. On the contrary, except for the [45°] angle of incidence, specimen f2 revealed a lower impact perforation failure in the knife width direction compared to other fabric specimens. This is due to the involvement of higher surface contact of the knife edge in the grinding direction with the fabric while perforation. This results in a higher amount of exerted energy concentrated on the specified area in which lower fabric surface or number of yarns are involved to distribute and absorb the impact energy. However, when the same fabric specimen is tested for different angles of incidence, the 2D fabric specimen barely shows significant difference among the various angles of incidence. It can also be inferred from the images of fabrics post impact that higher number of yarns are both pulled out and then faced yarn rupture in case of the different 3D woven fabric compared to 2D fabric specimen regardless of angle of incidences. This is due to the involvement of binding warp yarn in 3D woven fabric, which exhibits more deformation at the back before being cut by the knife, unlike the 2D plain woven fabric. A knife blade will cut the constituent yarns of the protective fabric during penetration, which can relate to more shearing than tensile properties of the yarn. Due to this, within the different 3D woven fabrics (f1, f2, and f3), the higher involvement of binding yarn composition results in more tensile deformation than shearing properties. In other words, the orientation of the binding warp yarns in the 3D woven structure is more closely aligned with the direction of the knife than the stuffer and weft yarns, resulting in reduced resistance to shear. Furthermore, the friction coefficient between the binding warp yarns and the knife blade is low, thereby not significantly contributing to the absorption of impact energy. As a result, f1 which constitutes all binding yarn in warp yarn system exhibit higher amount of yarn pullout and shearing followed by f2, a fabric with equal composition of binding and stuffer yarn in warp yarn system. Whereas, 3D woven fabric, f3 shown less yarn pull out and then shearing due to the involvements of higher amount of stuffer yarn as compared to binding yarn in their warp yarn system. In this case, the fibers are cut immediately while facing the knife where you will see a lot of fibrillated yarns on the failure area. Furthermore, it is seen from Fig. 9, corresponding to 3D and 2D woven fabric, that the post impact failure mode of the fabric at [45°] angle of incidence was exclusively complete cutting of the yarn, with lesser yarn pullout and fibrillation. In contrast, at both [0°] and [22.5°] angle of incidence, the post impact failure mode of the fabric showed both yarn pullout and fibrillation.

4.2. Effect of angle of incidence with different panel layer on stab performances of 2D/3D fabric

It is known that as the higher number of layers involved in the protective panel, the higher stab protection will be achieved while stabbing, particularly at perpendicular direction [0°] angle of incidence. However, it is not yet investigated how the number of layers involved within the protective panels behaves while stabbed at different angles of incidences. This section will discuss the effects of different angle of incidence, [0°], [22.5°], and [45°] while stabbing the single and four panels of the different 3D fabric types (f1, f2, and f3) and 5 layers (equivalent to one panel of 3D fabric specimen in areal density) to 20 layers of 2D fabrics (2D) (equivalent to four panels of 3D fabric specimen in areal density). Fig. 11 shows the effect of different stabbing angle of incidence [0°], [22.5°], and [45°] on the maximum surface trauma both in the knife width (X_{max}) and thickness (Y_{max}) direction of different tested specimens made with a single and four panels of 2D and 3D fabrics. As shown in Fig. 11, the values of the surface trauma in the knife width (X_{max}) direction show higher values as compared to the knife thickness (Y_{max}) direction regardless of the angle of incidences and type of fabric involved. However, except for Y_{max} values of specimen 2D, f1, and f2 tested at [22.5°] angle of incidence, the values of the trauma on both knife directions revealed higher values as the number of layers involved became higher for the different fabric type specimens. This is because, most of the strike energy has been directly absorbed by the specimen and distributed in larger surface area when involved higher number of layers. On the contrary, in the lower number of layer involvement, it is obvious that the impact energy faced lower contact areas and smaller amounts of fibers while passing through the fabric which resulted more penetration rather than creating trauma on the surface. The angle of incidence also has a significant impact on the values of the surface trauma marked on the plastiline at the back with different fabric specimens. Specifically, except specimen f3, other specimen 2D, f1, and f2 made with single panels of their respective fabric types revealed higher surface trauma value of 30, 22, and 20 mm respectively in knife thickness direction, Y_{max}, at [22.5°] angle of incident as compared to 0 and [45°] angle of incidence.

As the number of panels increased to four for the tested specimens, the maximum surface trauma values in knife thickness, Y_{max} were recorded as 35, 35, and 40 mm for 2D, f1 and f3 specimens respectively at 0° angle of incident. Like the Y_{max}, the maximum surface trauma measurement in knife width, X_{max} was recorded as 36, 32, 33, and 31 mm for the 2D, f1, f2, and f4 specimen respectively at a [22.5°] angle of incidence. On the contrary, as the number of layers increases, its surface trauma was measured as 40, 40, 35, and 50 mm for 2D, f1, f2, and f4 specimens respectively at [0°] angle of incidence. In general, the linear measurements of the maximum surface trauma width, X_{max}, created on the back of the tested specimens were found to be higher as the number of panels involved in the test specimens increases for different angles of

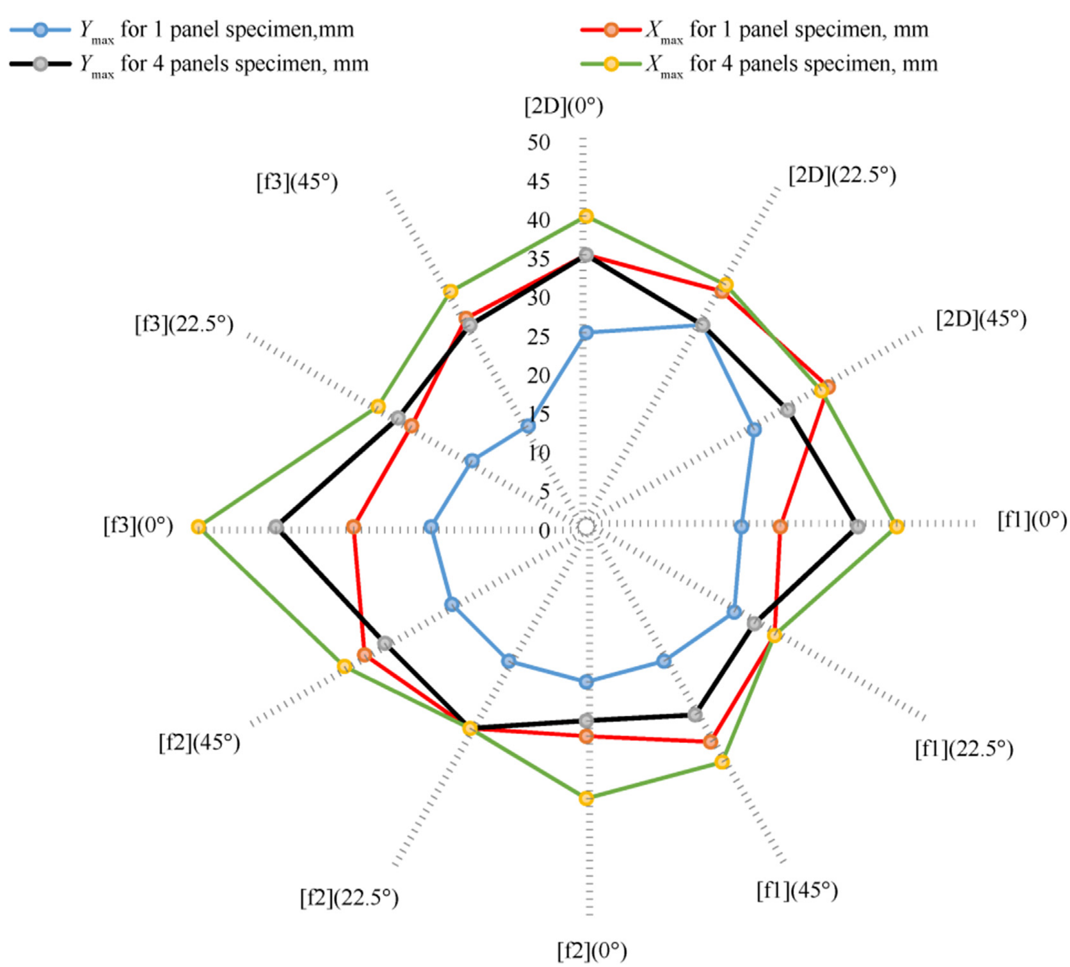

Fig. 11. The maximum surface trauma width on the surface of the backing material both in the blade thickness (Y) and blade width (X) direction while testing the four panels of different fabric specimen.

incidence. This is because, as the number of layers increases, the tendency of the specimen to absorb energy will be higher, dissipating the energy over wider areas of the fabric surface, resulting in higher trauma surfaces on the back of the materials, particularly on the plastiline. On the contrary, the maximum surface trauma thickness, Y_{max}, shows no or very small increments in most of the specimens as the number of panels involved in the test specimen and angle of incidence varies. This is due to the knife contacting the materials and penetrating only based on the thickness of the knife.

Figs. 12(a) and 12(b) show the values of the Depth of Trauma (DOT) and Depth of Penetration (DOP) respectively for various tested specimens, made of single and four panels, at different angles of incidence. The results indicate that the number of layers involved in the tested specimen and the angle of incidence have a significant impact on both the depth of trauma and depth of penetration values. For instance, target specimens made with four panel layers generally revealed lower values of both depth of trauma and depth of penetration compared to specimens with single panel layers, regardless of the angle of incidence. In general, the results show that as the angle of incidence increases, the values of the depth of trauma (DOT) become higher for all tested specimens. This means that the [0°] angle of incidence shows the lowest values, whereas the [45°] angle of incidence reveals the highest values of depth of trauma for all tested specimen types. For example, specimen 2D made with single and 4-panel fabric shows the depth of trauma values of [8 and 6.5 mm], [20 & 9 mm], and [21 & 9.5 mm] while tested against [0°], [22.5°], and [45°] angles of incidence respectively. Similarly, specimen f3 recorded [9 & 4 mm], [10 & 5 mm], and [11.5 & 10 mm] for [0°], [22.5°], and [45°] angles of incidence respectively for both single and 4-panel specimens. This is because the surface of the knife facing in contact with the fabric will be lesser and consequently more striking energy will be absorbed before creating a trauma at the back of the materials. On the other hand, the maximum depth of penetration (DOP) was recorded higher when the specimen was struck at the [0°] angle of incidence followed by the [45°] angle of incidence for all fabric specimens made with single panels. Whereas all specimens struck by the [22.5°] angle of incidence show the minimum values of DOP. For specimens made with 4-panels of fabrics, except for target specimen made with f2 fabrics, the depth of penetration shows a similar trend of single panel specimen for its striking angle. For example, specimen 2D noted the depth of penetration values of [26 & 12 mm], [7.6 & 4.28 mm], and [16.63 and 7 mm] for [single and 4-panels] while struck against [0°], [22.5°], and [45°] angles of incidence respectively. Similarly, specimen f1 and f3 made with single and 4-panel fabric recorded [37 & 14 mm], [12.35 & 5.23 mm], [21 & 7 mm] and [26 & 6 mm], [11.88 & 5.7 mm], [21 & 9.6 mm] for [0°], [22.5°], and [45°] angles of incidence respectively.

The increments of depth of penetration at the [0°] angle of incidences is since most of the striking energy will be concentrated within the limited fabric surface while passing through. This makes the fabric specimen have a lower tendency of dissipating and absorbing the striking energy to other fabric surfaces.

The length of penetration (LOP), like the depth of trauma and penetration, can also impart significant damage at the rear of the materials during stabbing events. This penetration length was carefully measured along the knife's edge and systematically analyzed across all tested fabric specimens, made with both single and four-panel layers. As shown in Fig. 13, irrespective of the fabric type used (2D and 3D woven fabrics) and angle of incidence ([0°], [22.5°], and [45°]), the measured LOP through backing materials/plastiline exhibited a visible decline as the number of panels involved in the specimen increased. For instance, at a [0°] angle of incidence, specimen 2D, f1, f2, and f3 made with [single and four-panel] registered length of penetration values of [20 and 9.35 mm], [30 and 15 mm], [22.5 and 10 mm], and [27.5 and 5 mm], respectively. This phenomenon arises from the higher resistance encountered by the knife when traversing through an increased number of panels to create the penetrations length at the rare of the tested specimens, like the depth of penetrations (DOP). Additionally, the angle of incidence also exerts a notable influence on the measured LOP values for varying specimens. Stabbing tests at a [0°] angle of incidence evinced the minimal LOP, succeeded by [45°] and [22.5°] for all single-panel fabrics specimens. However, with an increased number of panels in the tested specimen, some interesting outcomes results were recorded. For instance, specimen 2D and f3 exhibited a congruent trend as the number of panels increased, resulting in a higher LOP achieved at [22.5°], followed by

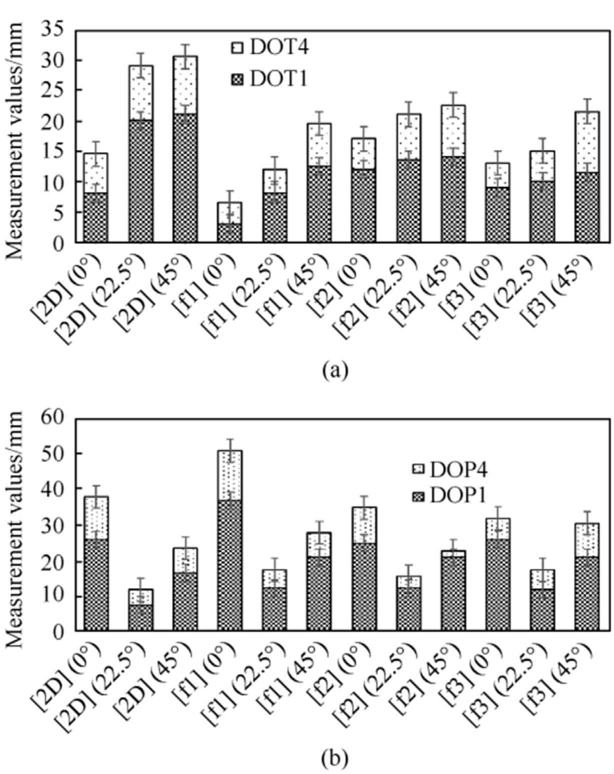

Fig. 12. The maximum (a) depth of trauma (dot) and (b) depth of penetration (DOP) for single and four panels of specimens made of different fabric structure tested at specific angle of incidences ([0°], [22.5°], and [45°]).

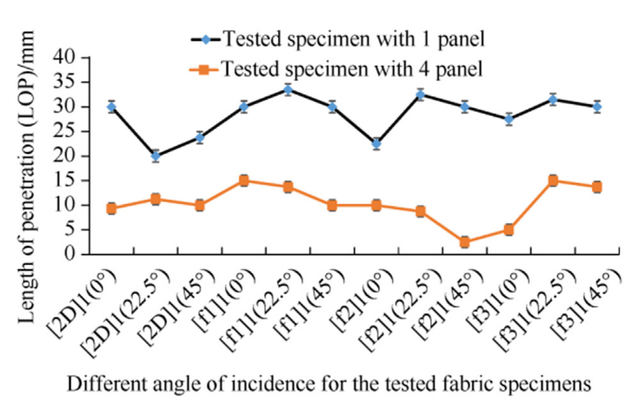

Fig. 13. The maximum Length of Penetration for single and four panels of specimens made of different fabric structure tested at specific angle of incidences ([0°], [22.5°] and [45°]).

[45°] and [0°]. This phenomenon occurs when the knife's mass drop line at this striking angle of incidence traverses in a direction where fewer yarn densities are engaged within the structure, thereby diminishing the likelihood of contacting, severing, and cutting more fibers by the knife. Conversely, both specimens f1 and f2 manifested a higher LOP at [45°], succeeded by [22.5°] and [0°] angle of incidence. This indicates a prevalence of greater depth of penetration than length of penetration at [0°] angle of incidence for all specimens. Furthermore, the fabric types also had a discernible influence on the LOP created at the backing materials/plastiline's rear when tested at varied angle of incidences. For instance, at all angles of incidence, 2D fabric specimen, (2D) showed minimal LOP values compared to other specimens made with 3D fabric, namely f1, f2, and f3, especially for specimens comprising single panels. On the contrary, specimen f1 exhibited the maximum LOP value for both single and multi-panel compositions compared to all other specimens at [0°] angle of incidence. This divergence arises from the compositions of specimen f1's 3D woven fabrics, comprising solely binding warp yarn, thereby conferring minimal stiffness and shearing resistance to the structure. Conversely, when the striking angle of incidence goes from [0°] to [45°] and number of panels increased, specimen f2 exhibited the minimal LOP followed by specimen 2D, f1, and f3 sequentially. This trend stems from the incorporation of balanced binding and stuffer warp yarn within the specimen f2's 3D fabric structure, augmenting its resilience against knife strikes from varying angle of incidences.

5. Conclusions

Various research studies have investigated the effects of various endogenous (material type and properties, fabric type and structure, chemical treatment, coating, etc.) and exogenous (testing conditions, impact velocity and energy, blade shape etc.) parameters on the stabbing capabilities of protective clothing. However, based on the author's knowledge, no study has investigated the effect of different angles of incidence on stab response and performance of different types of protective textiles. Current research has studied the stab response and performances of different structures of 3D WIFs and 2D high-performance fabric tested at [0°], [22.5°] and [45°] angle of incidence using a new stab experimental setup and measurement system. The results offer crucial insights into how varying angles of attack influence the protective fabric's ability to withstand and mitigate stabbing forces. Some conclusions are drawn as follows:

- As the angle of incidence increases, there is a noticeable escalation in the DOP inflicted on the tested fabrics, suggesting that higher angles of incidence result in greater trauma, indicating a reduced ability to absorb and distribute the impact energy efficiently.
- The specimens face a significant risk of puncture and higher DOP when subjected to both perpendicular angle of attack ([0°]) and high acute angles of incidence ([45°]). On the contrary, the DOP was consistently lower regardless of the fabric types at [22.5°] angle of incidence.
- The LOP was found to be lower for 2D fabric specimen as compared to all other three 3D WIFs specimens, f1, f2 and f3 for their respective angle of incidences. The result reveals that the LOP value was found higher at a slight acute angle of attack, [22.5°] angle of incidence, compared to other angle of incidences irrespective of fabric types.
- The measured LOP values at the backing materials also exhibited a visible decline as the number of panels involved in the specimen increased with irrespective of the fabric type used (2D and 3D WIFs) and angle of incidence ([0°], [22.5°], and [45°]) applied.
- The specimens made with higher panel layers revealed lower DOT and DOP values compared to lower panel specimen, regardless of the angle of incidence.
- The values of the DOT become higher as the angle of incidence increases for all types of tested specimens, whereas [0°] and [45°] angle of incidence show lowest and highest values of DOP for all tested specimen types.
- The composition of yarn within the warp yarn system also significantly affects the impact performance of various 3D woven fabrics at certain angles of incidence. For example, although all the 3D woven fabrics show insignificant differences at [22.5°] and [45°], the impact behavior of the f2 fabric (made of 50% stuffer yarns and 50 % binding yarns in the warp yarn system) demonstrates higher stab performance than the f1 fabric (composed of 100% binding yarns in the warp yarn system) at [22.5°] angle of incidence. This is attributed to the inclusion of stuffer warp yarns within the structure, which tends to increase stabbing performance likely due to higher friction and shear resistance combined with a different dynamic deformation behavior of the 3D woven architecture.
- Finally, the outcome of the result offers valuable insights and helps for stab protective textile designers and manufacturer, armor developer and stab testing and standardizing organizations to consider the angle of incidence while developing, testing, optimizing, and using protective textiles in various applications.

Declaration of interests

The authors declare that they have no known competing financial interests or personal relationships that could have appeared to influence the work reported in this paper.

CRediT authorship contribution statement

Mulat Alubel Abtew: Writing – review & editing, Writing – original draft, Visualization, Software, Methodology, Investigation, Formal analysis, Data curation, Conceptualization. **François Boussu:** Writing – review & editing, Validation, Supervision, Resources, Methodology, Data curation, Conceptualization. **Irina Cristian:** Writing – review & editing, Visualization, Validation, Supervision, Software, Data curation.

References

[1] Sitotaw DB, Ahrendt D, Kyosev Y, Kabish AK. A review on the performance and comfort of stab protection armor. Autex Res J 2022;22(1):96–107. https://doi.org/10.2478/aut-2021-0013.
[2] Abtew MA. A comprehensive review on advancements, innovations and applications of 3D warp interlock fabrics and its composite materials. Composites Part B 2024;278(June):111395. https://doi.org/10.1016/j.compositesb.2024.111395.
[3] Panneke N, Ehrmann A. Stab-resistant polymers—recent developments in materials and structures. Polymers 2023;15(4). https://doi.org/10.3390/polym15040983.
[4] Cheeseman BA, Bogetti TA. Ballistic impact into fabric and compliant composite laminates. Compos Struct 2003;35(18):161–73. https://doi.org/10.1016/S0263-8223(03)00029-1.
[5] Bilisik K. Two-dimensional (2D) fabrics and three-dimensional (3D) preforms for ballistic and stabbing protection: a review. Textil Res J 2016;87(18):2275–304. https://doi.org/10.1177/0040517516669075.
[6] Nayak R, et al. Body armor for stab and spike protection , Part 1 : Scientific literature review. Textil Res J 2017;0(00):1–21. https://doi.org/10.1177/0040517517690623.
[7] Rice K, Higgins KM, Boyd DG, U.S. Department of Justice. Stab resistance of personal body armor NIJ standard–0115.00. National Institute of Justice; 2000. p. 2000.
[8] Croft J, Longhurst D. HOSDB body armour standards for UK police. Part 3: knife and spike resistance. 2007. no. 39. 2007.
[9] Horsfall I, Watson C, Champion S, Prosser P, Ringrose T. The effect of knife

handle shape on stabbing performance. Appl Ergon 2005;36(4):505–11. https://doi.org/10.1016/j.apergo.2004.12.001. SPEC. ISS.
[10] Chadwick EKJ, Nicol AC, Lane JV, Gray TGF. Biomechanics of knife stab attacks. Forensic Sci Int 1999;105(1):35–44. https://doi.org/10.1016/S0379-0738(99)00117-6.
[11] Miller SA, Jones MD. Kinematics of four methods of stabbing: a preliminary study. Forensic Sci Int 1996;82(2):183–90. https://doi.org/10.1016/0379-0738(96)01994-9.
[12] Horsfall I, Prosser PD, Watson CH, Champion SM. An assessment of human performance in stabbing. Forensic Sci Int 1999;102(2–3):79–89. https://doi.org/10.1016/S0379-0738(99)00055-9.
[13] Kemp SE, Carr DJ, Kieser J, Niven BE, Taylor MC. Forensic evidence in apparel fabrics due to stab events. Forensic Sci Int 2009;191(1–3):86–96. https://doi.org/10.1016/j.forsciint.2009.06.013.
[14] Tien DT, Kim JS, Huh Y. Evaluation of anti-stabbing performance of fabric layers woven with various hybrid yarns under different fabric conditions. Fibers Polym 2011;12(6):808–15. https://doi.org/10.1007/s12221-011-0808-7.
[15] Das J, Singh Butola B, Majumdar A. Failure analysis of high-performance woven fabrics during quasistatic stabbing. Eng Fail Anal 2023;151(September):107385. https://doi.org/10.1016/j.engfailanal.2023.107385.
[16] Mulat AA, Boussu F, Bruniaux P, Loghin C, Cristian I. Engineering of 3D warp interlock p-aramid fabric structure and its energy absorption capabilities against ballistic impact for body armour applications. Compos Struct 2019;225(January):111179. https://doi.org/10.1016/j.compstruct.2019.111179.
[17] Abtew MA, Boussu F, Bruniaux P, Loghin C, Cristian I. Enhancing the ballistic performances of 3D warp interlock fabric through internal structure as new material for seamless female soft body armor development. Appl Sci 2020;10(4873):1–19.
[18] Abtew MA, Boussu F, Bruniaux P, Liu H. Fabrication and mechanical characterization of dry three-dimensional warp interlock para-aramid woven fabrics: experimental methods toward applications in composite reinforcement and soft body armor. Materials 2020;13(19). https://doi.org/10.3390/MA13194233.
[19] Chen X, Zahid B, Chen X. Impact evaluation of Kevlar-based angle- interlock woven textile composite structures. J Reinforc Plast Compos 2013;32(12):925–32. https://doi.org/10.1177/0731684413480006. October.
[20] Abtew MA, Boussu F, Bruniaux P, Loghin C, Cristian I. Effect of structural parameters on the deformational behaviors of multiply 3D layer-by-layer angle-interlock para-aramid fabric for fiber-reinforcement composite. J. Compos. Sci. 2020;4(4):145. https://doi.org/10.3390/jcs4040145.
[21] Chen X, Lo W-Y, Tayyar AE, Day RJ. Mouldability of angle-interlock woven fabrics for technical applications. Textil Res J Mar. 2002;72(3):195–200. https://doi.org/10.1177/004051750207200302.
[22] Nawab Y, Legrand X, Koncar V. Study of changes in 3D-woven multilayer interlock fabric preforms while forming. J Text Inst 2012;103(12):1273–9. https://doi.org/10.1080/00405000.2012.676267.
[23] Li M, Wang P, Boussu F, Soulat D. Investigation of impact performance of 3-dimensional interlock polymer fabrics in double and multi-angle pass stabbing. Mater Des 2021;206:109775. https://doi.org/10.1016/j.matdes.2021.109775.
[24] Li M, Boussu F, Soulat D, Luo J, Wang P. Impact resistance of pre-deformed stab of multi-ply three-dimensional interlock polymeric fabrics. J Ind Text 2022;51(3_suppl):4818S–41S. https://doi.org/10.1177/15280837221084363.
[25] Xuhong M, Xiangyong K, Gaoming J. The experimental research on the stab resistance of warp-knitted spacer fabric. J Ind Text 2012;43(2):281–301. https://doi.org/10.1177/1528083712464256.
[26] Alpyildiz T, Rochery M, Kurbak A, Flambard X. Stab and cut resistance of knitted structures : a comparative study. Textil Res J 2011;81(2):205–14. https://doi.org/10.1177/0040517510383617.
[27] El Messiry M, Eltahan E. Stab resistance of triaxial woven fabrics for soft body armor. J Ind Text 2014;0(00):1–21. https://doi.org/10.1177/1528083714551441.
[28] Reiners P, Kyosev Y, Schacher L, Adolphe D, Küster K. Experimental investigation of the influence of wool structures on the stab resistance of woven body armor panels. Textil Res J 2016;86(7):685–95. https://doi.org/10.1177/0040517515596934.
[29] El Messiry M. Investigation of puncture behaviour of flexible silk fabric composites for soft body armour. Fibres Text East Eur 2014;22(5107):71–6.
[30] Huh Y, Tien DT, Kim JS. Stab-resistant property of the fabrics woven with the aramid/cotton core-spun yarns. Fibers Polym 2010;11(3):500–6. https://doi.org/10.1007/s12221-010-0500-3.
[31] Cowper EJ, Carr DJ, Horsfall I, Fergusson SM. The effect of fabric and stabbing variables on severance appearance. Forensic Sci Int 2015;249:214–24. https://doi.org/10.1016/j.forsciint.2015.01.024.
[32] Wang D, Li J, Jiao Y. Stab resistance of thermoset-impregnated UHMWPE fabrics. Adv Mater Res 2010;139–141:133–6. https://doi.org/10.4028/www.scientific.net/AMR.139-141.133.
[33] Kim H, Nam I. Stab resisting behavior of polymeric resin reinforced p-aramid fabrics. J Appl Polym Sci 2012;123:2733–42. https://doi.org/10.1002/app.
[34] Hou L, Sun B, Gu B. An analytical model for predicting stab resistance of flexible woven composites. Appl Compos Mater 2013;20(4):569–85. https://doi.org/10.1007/s10443-012-9289-0.
[35] Her SC, Lai CY. Dynamic behavior of nanocomposites reinforced with multi-walled carbon nanotubes (MWCNTs). Materials 2013;6(6):2274–84. https://doi.org/10.3390/ma6062274.
[36] Bajya M, Majumdar A, Butola BS, Mawkhlieng U, Bhattacharjee D. Parametric optimisation of shear thickening fluid treatment for ultra-high molecular weight polyethylene woven fabric. J Ind Text 2022;52:1–22. https://doi.org/10.1177/15280837221126740.
[37] Hasanzadeh M, Mottaghitalab V. The role of shear-thickening fluids (STFs) in ballistic and stab-resistance improvement of flexible armor. J Mater Eng Perform 2014;23(4):1182–96. https://doi.org/10.1007/s11665-014-0870-6.
[38] Gürgen S, Kuşhan MC. The stab resistance of fabrics impregnated with shear thickening fluids including various particle size of additives. Composer Part A Appl Sci Manuf 2017;94(2017):50–60. https://doi.org/10.1016/j.compositesa.2016.12.019.
[39] Liu H, Fu K, Cui X, Zhu H, Yang B. Shear thickening fluid and its application in impact protection: a review. Polymers May 2023;15(10):2238. https://doi.org/10.3390/polym15102238.
[40] Obradović V, et al. Nanomechanical and anti-stabbing properties of Kolon fabric composites reinforced with hybrid nanoparticles. Composites Part B 2017;108:143–52. https://doi.org/10.1016/j.compositesb.2016.09.095.
[41] Abtew MA, Boussu F, Bruniaux P. Dynamic impact protective body armour: a comprehensive appraisal on panel engineering design and its prospective materials. Def. Technol. 2021;17(6):2027–49. https://doi.org/10.1016/j.dt.2021.03.016.
[42] V Hosur M, Jr JBM, Wetzel E, Jeelani S. Studies on the fabrication and stab resistance characterization of novel thermoplastic-kevlar composites. Solid State Phenom 2008;136:83–92. https://doi.org/10.4028/www.scientific.net/SSP.136.83.
[43] Mayo JB, Wetzel ED, Hosur MV, Jeelani S. Stab and puncture characterization of thermoplastic-impregnated aramid fabrics. Int J Impact Eng 2009;36(9):1095–105. https://doi.org/10.1016/j.ijimpeng.2009.03.006.
[44] Fahool M, Sabet AR. Parametric study of energy absorption mechanism in Twaron fabric impregnated with a shear thickening fluid. Int J Impact Eng 2016;90:61–71. https://doi.org/10.1016/j.ijimpeng.2015.11.016.
[45] Majumdar A, Laha A, Bhattacharjee D, Biswas I. Tuning the structure of 3D woven aramid fabrics reinforced with shear thickening fluid for developing soft body armour. Compos Struct 2017;178:415–25. https://doi.org/10.1016/j.compstruct.2017.07.018.
[46] He Q, Cao S, Wang Y, Xuan S, Wang P, Gong X. Impact resistance of shear thickening fluid/Kevlar composite treated with shear-stiffening gel. Composer Part A Appl Sci Manuf 2018;106:82–90. https://doi.org/10.1016/j.compositesa.2017.12.019.
[47] Li W, Xiong D, Zhao X, Sun L, Liu J. Dynamic stab resistance of ultra-high molecular weight polyethylene fabric impregnated with shear thickening fluid. Mater Des 2016;102:162–7. https://doi.org/10.1016/j.matdes.2016.04.006.
[48] Gong X, Xu Y, Zhu W, Xuan S, Jiang W, Jiang W. Study of the knife stab and puncture-resistant performance for shear thickening fluid enhanced fabric. J Compos Mater 2014;48(6):641–57. https://doi.org/10.1177/0021998313476525.
[49] Decker MJ, Halbach CJ, Nam CH, Wagner NJ, Wetzel ED. Stab resistance of shear thickening fluid (STF)-treated fabrics. Compos Sci Technol 2007;67(3–4):565–78. https://doi.org/10.1016/j.compscitech.2006.08.007.
[50] Xu Y, Chen X, Wang Y, Yuan Z. Stabbing resistance of body armour panels impregnated with shear thickening fluid. Compos Struct 2017;163:465–73. https://doi.org/10.1016/j.compstruct.2016.12.056.
[51] Liu Z, et al. Rheological characterization and synergistic energy absorption under fluid – solid interaction of shear thickening gel/3D angle interlocking composites Polymer composites. Polym Compos 2024;April. https://doi.org/10.1002/pc.28396.
[52] Santos T, et al. Effects of UV sensitivity and accelerated photo-aging on stab resistance of ρ-aramid fabrics impregnated with shear thickening fluids (STFs). Heliyon 2023;9(4):e15020. https://doi.org/10.1016/j.heliyon.2023.e15020.
[53] Nichols-Drew L, Armitage R, Hillman R, Sheridan K, Farrugia KJ. On a knife edge: a preliminary investigation of clothing damage using rounded-tip knives. Sci Justice 2020;60(6):495–503. https://doi.org/10.1016/j.scijus.2020.08.002.1.
[54] Zhang Q, Liu F, Wu D, Qu S, Liu W, Chen Z. A comprehensive understanding of knife cutting : effects of hardness , blade angle and the micro-geometry of blade edge on the cutting performance. Materials 2023;16(5375):1–17.
[55] Gong X, Xu Y, Zhu W, Xuan S, Jiang W, Jiang W. Study of the knife stab and puncture-resistant performance for shear thickening fluid enhanced fabric. J Compos Mater 2014;48(6):641–57. https://doi.org/10.1177/0021998313476525.
[56] Deleanu L, et al. The behaviour of stratified fabrics of aramid fibres under stabbing conditions. Polymers 2024;16(882):2–22.
[57] ASTM D 1777-96. Standard test method for thickness of textile materials. 2015. https://doi.org/10.1520/D1777-96R11E01. 10.1520/D1777-96R15.2.